Desalination and Water Treatment
www.deswater.com
49 (2012) 172–180
November

doi: 10.1080/19443994.2012.708228

Degradation of methylene blue adsorbed onto transparent adsorbent by UV-illumination (simple regeneration method)

Ahmad Baraka

Egyptian Armed Forces, Cairo, Egypt
Tel. +202 29283998; email: brkamtc@yahoo.com

Received 20 October 2011; Accepted 8 May 2012

ABSTRACT

This work presents in-pores degradation of a dye that was subjected to adsorption into a transparent adsorbent. The degradation was performed by UV-illumination of the dye-loaded adsorbent. This degradation by UV-illumination is considered as a regeneration technique for the adsorbent. For this specific aim, a new transparent adsorbent was prepared. It is a hybrid resin-gel composed of melamine formaldehyde tartaric acid/acrylamide tartaric acid (MFT/AT). methylene blue (MB) was selected as a typical contaminant dye due to its known degradability by UV rays. A sample of MFT/AT was used through 10-cycles of MB-adsorption/UV-illumination applying batch method. For each cycle, MB was apparently completely degraded. Rate of MB-adsorption by MFT/AT was investigated applying pseudo second order model for the 1st and 10th cycles. It was found that adsorption rate and capacity were not significantly changed (rate constants = 0.186, $0.199\,g\,mg^{-1}\,min^{-1}$ and capacities = 0.264, $0.258\,mg\,g^{-1}$ respectively). A fresh and the 10th-cycle-used samples of MFT/AT were characterized through Fourier transform infrared spectroscopy (FTIR), thermogravimetric analysis, Brunauer, Emmett and Teller method (BET) and scanning electron microscope to discover the side effect of UV-illumination on chemical, physical, morphological and aerial properties of adsorbent. It was found that MFT/AT was chemically and physically changed but its morphological and aerial properties did not change significantly.

Keywords: Transparent adsorbent; Regeneration; Degradation; Dye; UV-illumination

1. Introduction

Dyes represent a category of water pollutants which are discharged with wastewater effluents of several industrial processes, e.g. dye manufacturing, textiles dyeing, leathers, color printing, foods and drinks. Most of these dyes have a negative impact on aquatic life and human food resources. Consequently, remediation of wastewater effluent from these dyes at the point of origin is an important task. Currently, two famous remediation methodologies are frequently applied which are adsorption and photocatalytic degradation. For the first methodology, an adsorbent material is used to accommodate the dye within its pores. The rapidity of the adsorption process and the adsorbent capacity to accommodate the contaminant are essential key factors to consider [1]. The second methodology frequently employs UV-illumination of dye-water solution in the presence of TiO_2 suspension (anatase phase) to accelerate dye degradation.

There are some comments on these two methods. For the adsorption process, regeneration of adsorbent is economically important. However, regeneration is tedious, time-consuming and sometimes produces side waste. For TiO_2-suspension photocatalytic degradation, separating TiO_2 powder from treated water is also tedious and time-consuming. Several attempts

were conducted to enhance degradation *and to simplify* TiO_2 separation process from treated water, e.g. loading TiO_2 on a larger substrate [2], impregnating TiO_2 on active carbon [3], TiO_2-immobilization using binder [4], supporting TiO_2 on fibers [5], and supporting TiO_2 on silica gel [6].

To overcome the above mentioned comments, combining adsorption and photocatalytic degradation methods in one simultaneous process is a suitable approach when applying fixed bed column adsorption technique. By this combination, the photocatalytic degradation under UV-rays is considered as a tool to continuously regenerate the adsorbent. The adsorbent has to be transparent and impregnated by TiO_2. The scenario of continuous and simultaneous adsorption/regeneration process can be regarded as follows: (i) as wastewater flows through the column, the dye is adsorbed and trapped in the pores of the transparent adsorbent, (ii) during adsorption, the adsorbent is being UV-illuminated and because of adsorbent transparency the dye is subjected to UV-rays, (iii) due to presence of TiO_2 in adsorbent matrix, photocatalytic degradation will mineralize the dye, and (iv) consequently, the pores are evacuated from dye molecules which cause its readiness for successive *adsorption/degradation cycles*.

The idea of improvement comes from: (1) loading TiO_2 powder catalyst onto a transparent adsorbent cancels the need to separate TiO_2 from treated water and (2) due to continuous degradation and mineralization of dye in pores there is no need to stop the adsorption process for regenerating the adsorbent.

In this approach, adsorption itself is not a removal technique but it is considered as a tool to retain the dye contaminant in *the pores of the adsorbent* for a certain period of time. This period is sufficient enough for UV-illumination to degrade it and evacuate the pores (i.e. regeneration) for the subsequent quantity of dye to undergo the same process. As mentioned, the adsorbent must be transparent to accomplish the task.

To verify the above approach, a two-stage study was planned:

(1) The first stage includes the preparation of a transparent adsorbent, applying batch method for equilibrium-adsorption of a dye by this adsorbent and then exposing *the* dye-loaded adsorbent to UV-illumination to degrade the dye (through photolysis) as a regeneration step. In this stage, no TiO_2 is impregnated onto the adsorbent. This means that degradation is due to photolysis. The adsorption and regeneration will be assessed from batch point of view.

(2) The second stage includes the application of continuous adsorption technique using fixed bed column filled with grains of TiO_2-impregnated transparent adsorbent. During dye adsorption, the column *is being* exposed to UV rays for continuous regeneration. In this stage, adsorption and regeneration will be assessed considering the continuity of adsorption and regeneration.

The present work is dedicated to investigate the first stage only to verify the idea of degradation of a dye in the pores of the adsorbent and *to assess* the capability of adsorbent to re-adsorb again and again. This would suggest the proper application of adsorption/degradation-regeneration/re-adsorption cycles. Upon verification of this idea, the second stage will be carried out in a separate *future* work.

Beside the rapidity of adsorption process and reasonable adsorption capacity, this work requires a transparent adsorbent material for *the aim* of regeneration. For this aim, synthesis of a new hybrid transparent adsorbent (melamine formaldehyde tartaric acid/acrylamide tartaric acid [MFT/AT]) is introduced in the present work. The MFT part of the hybrid is a rigid-porous-hydrophilic resin which is able to adsorb dyes from wastewater [7,8]. Its removal ability was determined in preliminary experiments which are not presented here. It has some transparency but not clear enough to achieve the objective of the work. The AT part of the hybrid is a well known transparent gel material that easily swells water [9]. When combining MFT and AT in one hybrid system, the transparency *has been enhanced*. The transparency of MFT/AT gives the opportunity to apply the methodology of the mentioned degradation-regeneration cycles by illuminating the transparent MFT/AT with UV source.

Methylene blue (MB) (MW: $C_{16}H_{18}ClN_3S$, ($\lambda_{max.} \approx$ 660 nm) was selected in this study as a typical organic dye-pollutant. Its UV-degradation phenomenon is well known and had been accepted to follow in this study as it is believed that MB physically adsorbs onto MFT/AT surface and pores [10]. Simply, as MB (and many other organic dyes) is photodegradable in aqueous system when exposed to ultraviolet rays, *exposure* of MB-laden transparent adsorbent-grains to UV-illumination *should* cause degradation and mineralization of MB throughout the adsorbent material (outer surface, inner surface, and pores). Under continuous UV-illumination and as time elapses, MB will degrade and mineralize converting into primary components leaving the surface and pores of adsorbent-grains vacant and ready again for successive adsorption and degradation.

This study presents the MFT/AT preparation conditions and its characterization. It also shows the removing behavior of this adsorbent toward MB (rate and capacity), the regeneration of MFT/AT by UV-illumination and the effect of UV-illumination on MFT/AT material. Dye-adsorption using transparent adsorbent that is loaded with TiO_2 was studied [6]. However, there was no discussion about regeneration and reusability.

Although batch technique was applied in this study, it gives indication that an opportunity is available to upgrade the method by applying continuous fixed bed technique. In this technique dye-adsorption and UV-illumination-degradation *should be working simultaneously*. In this case there is no need to remove adsorbent-cartridge for regeneration process that is favored in many practical designs. This research will be performed in a future work.

2. Experimental

2.1. Chemicals and tools

The following chemicals were used to prepare the MFT/AT adsorbent: melamine (Aldrich), tartaric acid (Aldrich), acrylamide (Aldrich), formaldehyde 38% (BDH), conc. HCl (Sigma). For all preparations, deionised water was used. Conventional drying oven and gamma cell (Gamma Chamber 5000-India, Activity: 12000 curies 1998.) were used for the preparation processes. Hanna instrument-meter (H18519) was used to adjust the acidity of the initial solution of the hybrid mixture and to adjust the acidity of MB-solution. Stuart regular shaker was used for adsorption experiments.

2.2. Preparation of MFT/AT hybrid gel-resin adsorbent

MFT/AT was prepared using one-pot manner. The components [melamine (3.2 g), tartaric acid (4.5 g), acrylamide (1.4 g), and formaldehyde (6 ml)] were mixed together in a 50-ml vial containing 14 ml of pre-acidified water (pH = 1.5). The vial was kept tightly closed and introduced into a pre-heated drying oven at about 120˚C. A white dense slurry product was observed within 15 min which turned into a slightly viscous and transparent solution within about an hour. Directly after formation of that solution, the vial was transferred to the gamma cell to receive a dose of 2 KGy. A clear transparent solid material is produced and the vial was returned back to the drying oven for extra heating at about 90˚C for 6 h. The tightly closed vial containing the solid transparent MFT/AT was then removed from the oven and left on bench for about 18 h for more curing. Then, the sample was removed from the vial and ground. The produced grains were sieved and the 355–710 μm fraction was collected and washed seven times, each with 250 ml of hot (90˚C) deionised water for an hour to remove the residue reactants and to reduce acidity. After washing, the grains were left to cool for 30 min then washed again three times with deionised water. Afterwards, the excess water (non-sorbed) was removed by centrifugation. The washed sample was stored for planned adsorption.

Formation of the MFT resin-part of the hybrid follows the same mechanism presented in some previous works [7,8]. In brief: due to heating the initial mixture at 120˚C, MF matrix starts to form by condensation reaction, meanwhile the carboxylic groups (–COOH) of tartaric acid react with certain percentage of primary amine groups ($–NH_2$) of melamine *to form* amide covalent bonds. By transferring the sample into gamma cell, the known radiation-induced polymerization reaction of acrylamide with tartaric acid by gamma radiation occurs forming AT gel-part of the hybrid [9]. It is suggested that the product is two 3D-networks of MFT and AT which are inter-merged.

2.3. Instrumental analysis

IR spectra of the dried fresh and dried 10th-time regenerated MFT/AT samples were recorded in the range 400–4,000 cm^{-1} applying KBr-disc technique using a Perkin–Elmer FT-IR spectrometer. Field emission-scanning electron microscope (FE-SEM) was employed for imaging the outer surface of semi-dried grains of fresh and 10th-time regenerated MFT/AT to investigate their morphologies and apparent porosities (magnification: ×4000 and accelerating voltage: 25 and 21 kV). Semi-dried samples of fresh and 10th-time regenerated MFT/AT were used to determine their thermo-gravimetric curves. Thermogravimetric analysis (TGA) was carried out using Shimadzu TGA-50H under a continuous argon flow of 100 ml/min, heating from room temperature to 500˚C with 10˚C/min heating rate. Freeze-dried samples of fresh and 10th-time regenerated MFT/AT were used to determine their porosities applying Brunauer, Emmett and Teller method (BET) analysis technique using Micromeritics ASAP 2405N adsorption analyzer (nitrogen adsorption/desorption isotherms at 77.4 K).

2.4. Kinetics of MB-adsorption onto MFT/AT

Pseudo-second order model was applied to determine the kinetic parameters of MB-adsorption (rate

and capacity) from synthetic wastewater onto MFT/AT. This model was selected to be applied because of its wide applicability considering several different adsorption systems [10]. The model has the following known integral form [11]:

$$t/q_t = 1/(k_2 q_e^2) + t/q_e$$

where q_t and q_e (mg/g) are the amounts of MB adsorbed at time t and at equilibrium respectively. The parameter k_2 (g/mg min) is the adsorption rate constants. By plotting t/q_t vs. t, adsorption rate constant and capacity of MFT/AT can be determined *respectively* from the intercept and slope of regression line.

For any adsorption process, there are three solute-migration (diffusion) steps: bulk, film and intra-particle diffusions. The slowest step controls the total rate of adsorption. Intra-particle diffusion can be dedicated to be the rate-limiting step in batch studies [12]. As the pseudo-second order kinetic model cannot determine the diffusion mechanism and to investigate if film and/or intra-particle diffusions are controlling the adsorption process, the intra-particle diffusion model should be applied [13]:

$$q_t = k_i\, t^{0.5} + I$$

where slope k_i is the intra-particle diffusion rate constant and intercept I is related to the thickness of boundary layer and represents the film diffusion. By plotting q_t vs. $t^{0.5}$, intra-particle diffusion and film diffusion can be determined through the slope and intercept. Studying intra-particle diffusion in this work is important to investigate the effect of UV rays on MFT/AT internal morphology which can affect the kinetics of adsorption.

To apply both models, residual concentrations of MB were determined by measuring MB-solution absorbance at $\lambda_{max} = 660$ nm using Shimadzu UV–vis 1300. From these concentrations, corresponding q_t values were calculated. These measurements and kinetic determinations were performed for fresh and 10th-time regenerated samples.

2.5. Steps of adsorption and regeneration of MFT/AT by UV-illumination

Step 1, MB adsorption: 0.1 g of MFT/AT was treated by MB-solution (25 ml, 5 ppm and pH ≈ 6.5). Removal of MB was performed using shaker (70 rpm at ambient temperature ~ 22°C) for 6 h to guarantee equilibrium. Then, the MFT/AT grains (turned blue) were separated from solution for the next step.

Step 2, MFT/AT regeneration: The MB-treated MFT/AT sample was added to 100 ml of fresh distilled water and poured into a UV chamber. UV-illumination (lamp length: 25 cm, λ: 254 nm and power: 16 W) was powered for 72 h. By the end of this period, the sample became completely colorless indicating the degradation of MB from the sample.

Steps 1 and 2 were repeated 10 times using the same MFT/AT sample. As a control sample, 0.1 g of MFT/AT was treated by MB-solution and regenerated by only the same heat effect of UV-illumination (about 40°C) for the same period of time (72 h). Then, both samples were withdrawn from respective containers to evaluate the degradation of MB and regeneration of MFT/AT.

3. Results and discussion

3.1. Transparency of prepared samples

A fresh MFT/AT sample (monolithic piece of about 2-cm thickness) is shown in Fig. 1. It is apparent from the photo that MFT/AT has a transparency.

3.2. Kinetics of MB-adsorption on MFT/AT

Time profiles (180 min) of the MB-removal by fresh and 10th-time regenerated MFT/AT samples are shown in Fig. 2. For both samples, it can be *observed* that *removal behaviors are similar*. Each has two removal stages. The first is rapid and covers the first 15 min during which a considerable percentage of MB (about 75% of total removed) has been adsorbed for both samples. This percentage removal may be due to adsorption onto the outer surface/layer of MFT/AT

Fig. 1. Transparency of MFT/AT.

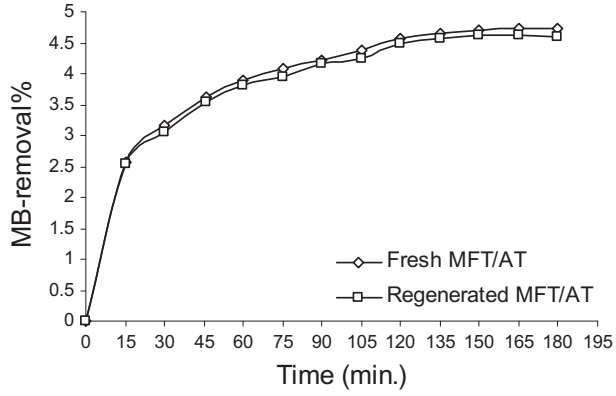

Fig. 2. Adsorption time profile (180 min) of MB onto fresh and 10-times regenerated MFT/AT.

grains. Next, a slow and smoothly increasing stage is observed where equilibrium is attained at the end. The second stage suggests a uniform adsorption process which depends on MB migration through MFT/AT pores. The similarity of the two plots may indicate that MFT/AT material of the 10th-time regenerated sample did not suffer considerable changes in its morphological and aerial properties after 10 times of UV-illumination. Hence, adsorption kinetic behavior would not significantly be affected by UV-illuminating MFT/AT.

Linear regression applying pseudo-second order model using experimental data of Fig. 2 was performed and plots are given in Fig. 3. From the plots, the model parameters were determined with corresponding correlation factors (r) and standard errors (SE). For both data sets, correlations were found significant and the linearity with 95%-confidence, given by the regression, was concluded according to analysis of slope and intercept values [14]. The standard errors of these parameters are comparatively low. Accordingly, pseudo-second order model can be

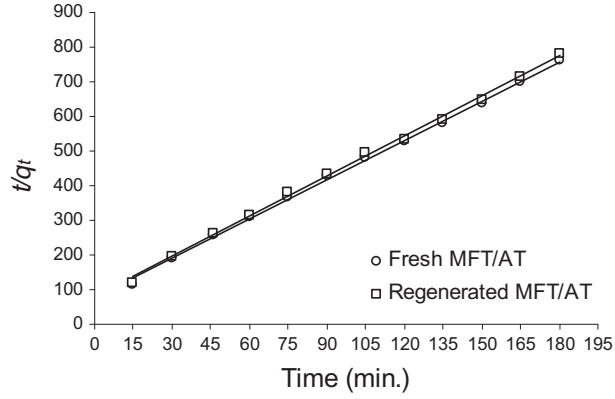

Fig. 3. Pseudo second-order plots of MB-adsorption onto fresh and 10-times regenerated MFT/AT.

Table 1
Pseudo second-order parameters of MB-adsorption on fresh and regenerated MFT/AT

Sample	k ($g\,mg^{-1}\,min^{-1}$)	q_e ($mg\,g^{-1}$)	r
Fresh MF-T/AT	0.186	0.264	0.9987
Used 10th-time regenerated MF-T/AT	0.199	0.258	0.9981

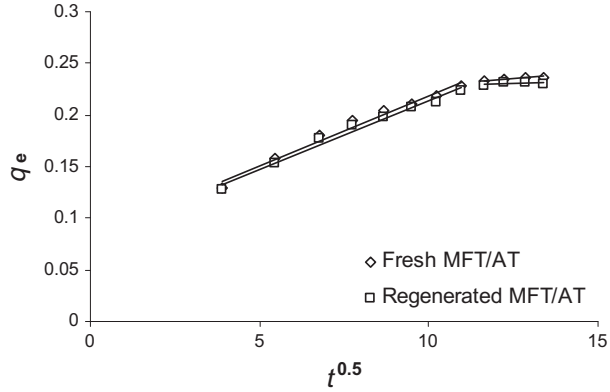

Fig. 4. Diffusion plots of MB-adsorption onto fresh and 10-times regenerated MFT/AT.

assigned to represent the entire removal process of MB by MFT/AT. It is believed that MB was physically adsorbed on MFT/AT surface following the proposal given by Plazinski et al. [10].

The rate constants and capacities are given in Table 1. From table, it is clear that regenerated sample has a slightly higher adsorption rate than that of the fresh sample. This may be due to some degradation that occurred for MFT/AT material itself by UV rays. This degradation slightly widened pores which facilitated migration of MB molecules through them. On the contrary, capacity of MFT/AT slightly decreased from 0.264 to $0.258\,mg\,g^{-1}$ after regeneration processes. This may be due to measured decrease in sur-

Table 2
Intra-particle diffusion parameters of MB-adsorption on fresh and regenerated MFT/AT

Sample	k_i ($mg\,g^{-1}\,min^{-0.5}$)	I	r
Fresh MF-T/AT	0.0136	0.0832	0.9808
Used 10th-time regenerated MF-T/AT	0.0133	0.0807	0.9818

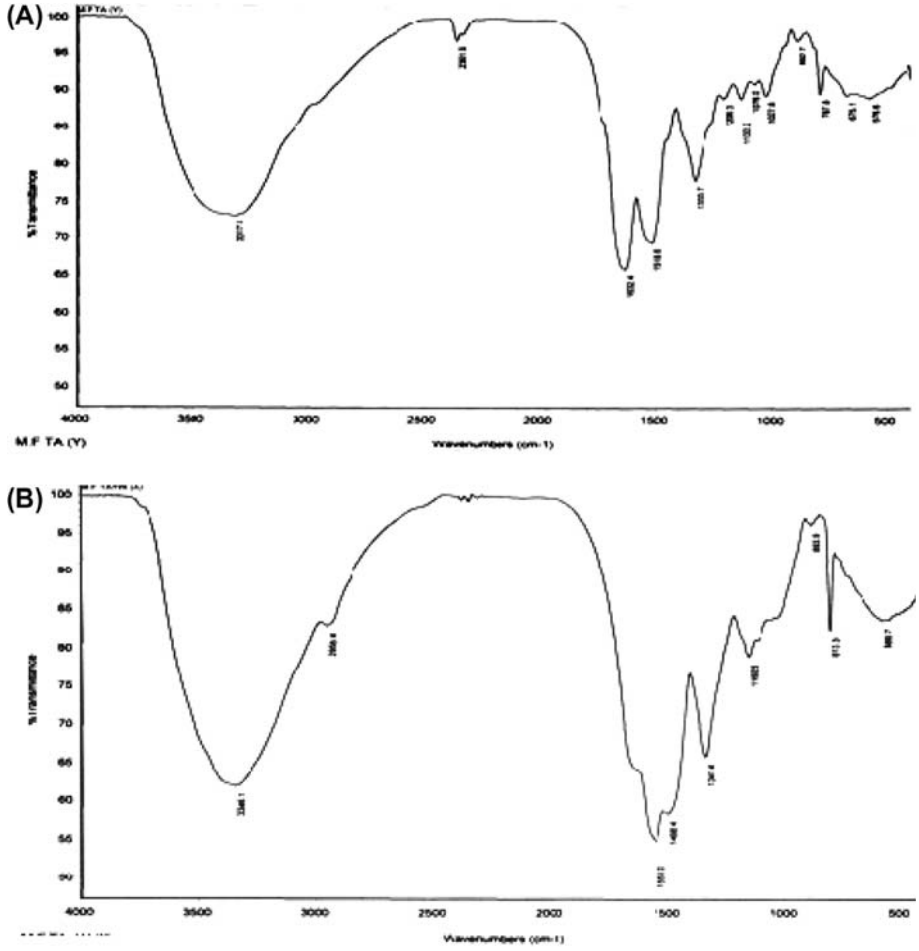

Fig. 5. IR spectra of (A) fresh MFT/AT and (B) 10th-cycle UV-illuminated MFT/AT.

face area from 36.5 to 33.4 $m^2 g^{-1}$ as it will be shown in the discussion of BET analysis.

Fig. 4 shows the plots (q_t vs. $t^{0.5}$) of diffusion of MB onto fresh and regenerated MFT/AT samples. As resistance during bulk diffusion can be neglected because of shaking action, adsorption stages can be attributed to film diffusion, intra-particle diffusion and binding [15]. Segmented linear regression of data points showed three distinct stages. The first one (lines are not drown) covers the first 15 min and represents the film diffusion where MB was instantaneously adsorbed onto the outer surface of MFT/AT grains [16]. The second stage is given by line covers the period 15–120 min representing intra-particle diffusion. The third stage covers the period 120–180 min which denotes equilibrium and its small slope is due to the low concentration of MB in this stage [15].

Table 2 gives the parameters of intra-particle diffusion model estimated for the second stage. The values of rate constant, k_i, are almost similar and this is true also for the values of film resistance, I. This indicates that

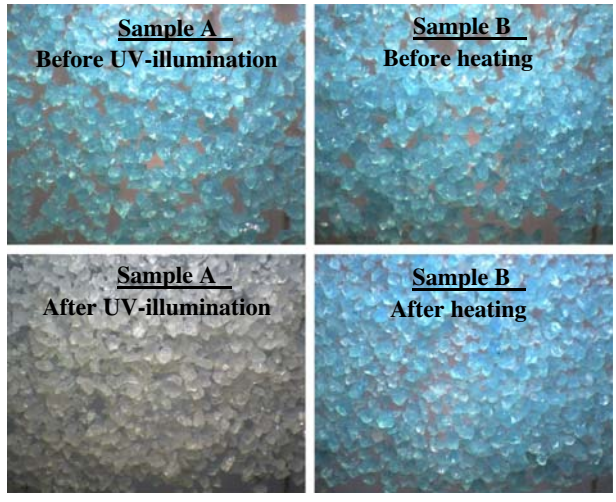

Fig. 6. Photographic images (×60 magnification) of (A) MFT/AT sample passes through 10 cycles of MB-adsorption and UV-illumination and (B) sample that was exposed only to the same temperature degree (40°C) as sample A.

adsorption behavior did not change considerably from the fresh sample to the regenerated one. According to Fig. 4 and Table 2, film diffusion (*I* values) is a step that has a control on the overall adsorption process.

In general, it is concluded that overall rate and capacity did not significantly change throughout 10 cycles of adsorption/regeneration processes. This means that MFT/AT adsorbent can withstand another several 10s of cycles without effective loss in removal capability.

3.3. Evaluation of regeneration of MFT/AT by UV-illumination

Fig. 5 shows the IR spectra of two samples. The first is for a fresh sample of MFT/AT and the second is for a sample that has suffered 10 cycles of MB-adsorption/regeneration. Considering the second sample (Fig. 6(B)), there are no peaks related to MB that can be assigned in the figure such as stretching vibration adsorption bands at 2,800–3,000 cm^{-1} and vibration attributed to methyl and benzene ring framework at 1,422 cm^{-1}. This indicates, almost, complete degradation of MB.

Fig. 6 may help to assign the success of MB-degradation inside MFT/AT pores. It gives the photographic images (×60 magnification) of two samples of the hybrid adsorbent. Sample (A) passes through 10 cycles of MB-adsorption and UV-illumination and as shown the sample is colorless after the 10th UV-illumination process which indicates almost complete degradation of MB inside MFT/AT pores. This in fact

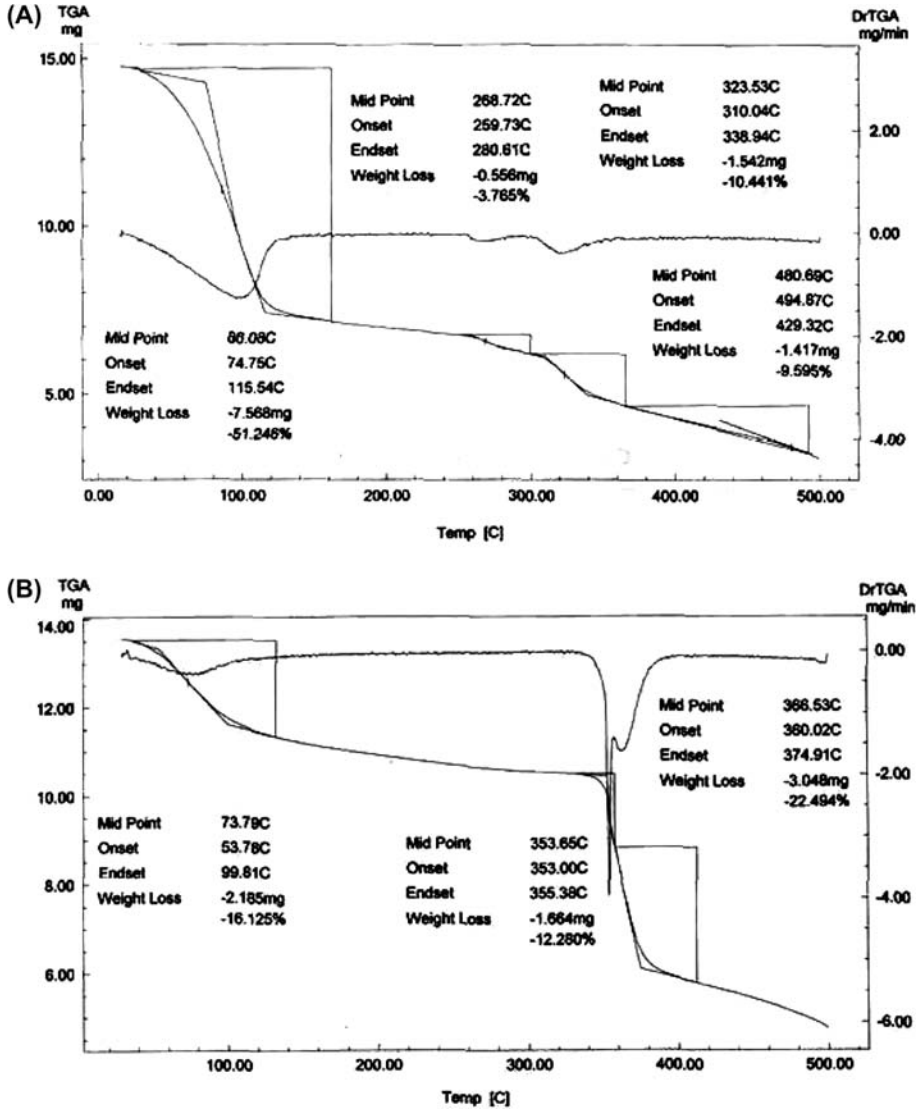

Fig. 7. Thermograph of (A) fresh MFT/AT and (B) 10th-cycle UV-illuminated MFT/AT.

Table 3
Data of TGA measurements for fresh MFT/AT and UV-illuminated MFT/AT

Character	Fresh MFT/AT				UV-illuminated MFT/AT		
	R1	R2	R3	R4	R1	R3	R4
Mid point (°C)	86	269	324	481	74	354	367
Onset (°C)	75	260	310	495	54	353	360
Endset (°C)	116	281	339	429	100	355	375
Weight loss (%)	54	3.8	10	10	16	12	22

is the reason why a subsequent adsorption process is possible. Sample (B) was exposed only to the same heat effect as sample (A) suffered in UV-illumination and a notable change in color is observed (the blue is less dense) which may be due to MB-thermal degradation only. It can be concluded that UV-illumination is effective for the degradation of MB inside MFT/AT pores.

It is important to mention that a period of 72 h was needed for each cycle to completely degrade MB by UV-illumination which is practically a long period. However, it is believed that impregnating MFA/AT with suitable amount of TiO_2 as a photocatalyst would significantly help to reduce this period. This factor will be considered in a future work.

3.4. Effect of UV-illumination on MFT/AT material

Comparing the IR spectra of fresh MFT/AT sample and 10th-time UV-illuminated MFT/AT sample (Fig. 6), some significant differences can be detected. The carbonyl part of amide group (1,632 cm^{-1}) became less strong for the regenerated sample. Peak at 1,492 cm^{-1} became stronger. Peak at 1,333 cm^{-1} was shifted to 1,341 cm^{-1} due to heating-morphological changes. Peaks at 1,206 and 1,133 cm^{-1} disappeared. Other some detailed peaks at lower wave-numbers became very weak to be detected. This obvious change in spectra suggests strong effect of UV-illumination on the functional groups of the adsorbent. That is, degradation occurred not only for adsorbed MB but also partially for MFT/AT matter itself. This means that a considerable part of UV-energy was consumed for adsorbent partial degradation causing change in its chemical structure.

Thermographs of two samples; fresh and 10th-time UV-illuminated MFT/AT, are shown in Fig. 7. Table 3 summarizes the data of these graphs. From the table, it is clear that each sample has its own scenario of losing mass. This may be due to matrix phase change of the second sample which occurred due to exposure to UV rays or its accompanying heat during the 10 times of treatment.

SEM images of MFT/AT surface before MB-adsorption and after 10 times of MB-adsorption/regeneration processes have been determined and shown in Fig. 8. It is clear from the figure that both images are almost similar. Both surfaces are irregular and highly configured and it seems that UV rays did not cause any observable morphological change.

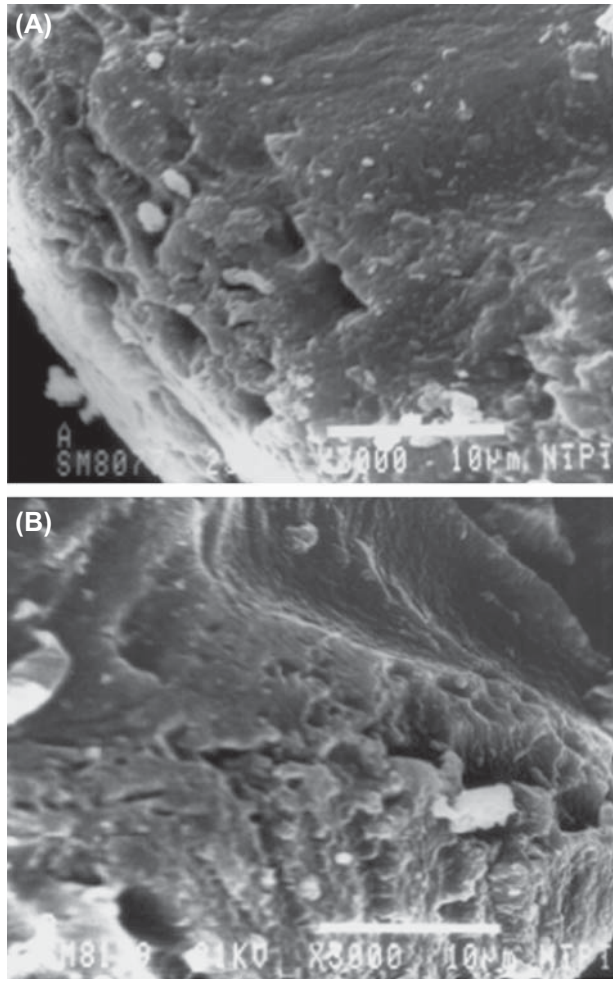

Fig. 8. SEM image of (A) fresh MFT/AT and (B) 10th-cycle UV-illuminated MFT/AT.

Table 4
Porosity characteristics of MFT/AT

Character	Fresh MFT/AT	10-cycle-used MFT/AT
Total BET surface area ($m^2 g^{-1}$)	36.5	33.4
BET micropores (<2 nm)	0.2	0.2
BJH adsorption cumulative pore volume ($cm^3 g^{-1}$)	0.083	0.093
Total average pore diameter (nm)	13.4	14.2

The outputs of BET analysis of MFT/AT before MB-adsorption and after 10 times of MB-adsorption/regeneration processes are given in Table 4. For each sample, surface area is limited and the same is true for cumulative pore volume. However, the average pore diameter (>13 nm) is suitable for dye drifting in pores (MB area: 132 $Å^2$). Micropores area has very small value and consequently meso- and macro- pores are suggested to be the dominant categories. The total surface area of regenerated sample ($33.4 m^2 g^{-1}$) is slightly lower than that of fresh sample ($36.5 m^2 g^{-1}$) and this may be due to some degradation of adsorbent.

From IR, TGA, SEM and BET analyses it can be concluded that although significant chemical and physical changes occurred to MFT/AT because of UV exposure, the morphology and total surface area did not suffer critical change. This is the reason of stable adsorption behavior of MFT/AT toward MB over 10 times of adsorption/regeneration processes.

4. Conclusion

A new transparent hybrid resin-gel adsorbent was prepared; MFT/AT. It was chemically designed to be able to adsorb dyes and in the same time can be regenerated by UV-illumination due to its transparency. It successfully passed 10 adsorption/regeneration cycles with almost kinetic-stable ability to remove MB. The adsorbent material was chemically and physically affected by UV-illumination with no critical effect on adsorption behavior due to stable morphological and aerial properties. The output of this study encourages the use of TiO_2-imprgnated MFT/AT or any other transparent adsorbent for removal of UV-degradable organic contaminants applying fixed bed column technique. It is suggested that adsorption/regeneration processes can be performed simultaneously in a continuous system which help in simplifying wastewater remediation technique and this subject will be considered in a near future work.

References

[1] S. Faust, O. Aly, Adsorption Processes for Water Treatment, Butterworths, Boston, MA, 1987.
[2] A. Saepurahman, M.A. Abdullah, F.K. Chong, Preparation and characterization of tungsten-loaded titanium dioxide photocatalyst for enhanced dye degradation, J. Hazard. Mater. 176 (2010) 451–458.
[3] A.K. Subramani, K. Byrappa, S. Ananda, K.M. Lokanatha, C. Ranganathaiah, M. Yoshimura, Photocatalytic degradation of indigo carmine dye using TiO_2 impregnated activated carbon, Bull. Mater. Sci. 30 (2007) 37–41.
[4] J. Kumar, Photocatalytic degradation of amaranth dye over immobilized nano-crystals of TiO_2, EE'10 Proceedings of the 5th IASME/WSEAS international conference on Energy & environment, 2010, pp. 129–133, ISBN: 978-960-474-159-5.
[5] N. Barka, A. Assabbane, A. Nounah, Y. Aît Ichou, Photocatalytic degradation of indigo carmine in aqueous solution by TiO_2-coated non-woven fibres, J. Hazard. Mater. 152 (2008) 1054–1059.
[6] Y. Chen, K. Wang, L. Lou, Photodegradation of dye pollutants on silica gel supported, TiO_2 particles under visible light irradiation, J. Photoch. Photobio. A 163 (2004) 281–287.
[7] A. Baraka, P. Hall, M. Heslop, Melamine–formaldehyde–NTA chelating gel resin: Synthesis, characterization and application for copper(II) ion removal from synthetic wastewater, J. Hazard. Mater. 140 (2007) 86–94.
[8] A. Baraka, P. Hall, M. Heslop, Preparation and characterization of melamine–formaldehyde–DTPA chelating resin and its use as an adsorbent for heavy metals removal from wastewater, React. Funct. Polym. 67 (2007) 585–600.
[9] E. Saraydin, O. Gűven, Swelling of acrylamide-tartaric acid hydrogel, Iranian journal of polymer science and technology 4 (2009) 219–225.
[10] W. Plazinski, W. Rudzinski, A. Plazinska, Theoretical models of sorption kinetics including a surface reaction mechanism: A review, Adv. Colloid. Interf. 152 (2009) 2–13.
[11] Y.S. Ho, G. McKay, Pseudo-second-order model for sorption processes, Process Biochem. 34 (1999) 451–465.
[12] N.K. Amin, Removal of direct blue-106 dye from aqueous solution using new activated carbons developed from pomegranate peel: Adsorption equilibrium and kinetics, J. Hazard. Mater. 165 (2009) 52–62.
[13] W.J. Weber, J.C. Morris, Kinetics of adsorption on carbon from solution, J. Santi. Eng. Div. ASCE 89(SA2) (1963) 31–59.
[14] J. Taylor, An introduction to error analysis, the study of uncertainties in physical measurements, 2nd ed., University Science Books, Sausalito, CA, 1997.
[15] S. Chen, J. Zhang, C. Zhang, Q. Yue, Y. Li, C. Li, Equilibrium and kinetic studies of methyl orange and methyl violet adsorption on activated carbon derived from Phragmites australis, Desalination 252 (2010) 149–156.
[16] D. Kavitha, C. Namasivayam, Experimental and kinetic studies on methylene blue adsorption by coir pith carbon, Bioresource Technology 98 (2007) 14–21.